Neutron Reflectivity of Linear−Dendritic Diblock Copolymer Monolayers

Mark A. Johnson, Catherine M. B. Santini, Jyotsna Iyer, Sushil Satija, Robert Ivkov, and P. T. Hammond*

Department of Chemical Engineering, Massachusetts Institute of Technology, 77 Massachusetts Avenue, Cambridge, Massachusetts 02139-4307

Received February 28, 2001; Revised Manuscript Received September 25, 2001

ABSTRACT: Specular neutron reflectivity has been used to investigate the structure of monolayers formed from linear−dendritic diblock copolymers at an air−water interface. The dendritic block copolymers consist of a linear poly(ethylene oxide) (PEO) block of 2000 molecular weight linked to a third or fourth generation polyamidoamine (PAMAM) dendron. The dendritic end groups were functionalized with deuterated stearic acid to make the dendritic block hydrophobic, resulting in a macroamphiphile. Results indicate that stable monolayers are formed with PEO resting on the subphase and stearate groups extending into the air. In general, at low surface concentrations the PEO block intermixes with the PAMAM dendron, whereas at high surface concentrations the PAMAM forms a distinct layer above the PEO. The ordering of the stearate groups functionalized on the dendrimer was dependent on generation. Stearate groups form a distinct ordered layer which is separate from the third generation PAMAM dendron, whereas the stearate groups are intermixed with fourth generation PAMAM segments due to the curvature of the higher generation dendron. The PEO block becomes intermixed with the water subphase if the monolayer is held at constant area for at least 10 h. These finding are consistent with earlier published studies of pressure−area isotherms of these systems on the Langmuir−Blodgett trough.

1. Introduction

A great deal of interest has been directed toward dendrimers, initially due to their novel molecular structure, and more recently due to spurred excitement regarding new practical uses for dendritic materials. These hierarchically branched materials consist of a central core, an interior region containing nanoporous cavities, and an outer molecular surface with end groups that can be functionalized with a large range of chemical groups.[1] The nanoporous cavities inside dendrimer molecules can be used to sequester ions and small molecules[2] or as templates for the formation of metal nanoparticles.[3,4] Functionalization of the dendrimer end groups can be used to alter the solubility, adhesive properties, or the diffusion rate in to and out of the molecule.[5−7]

Potential applications involving dendrimers include encapsulant coatings, magnetic storage media, and catalytic membranes. Dendrimers can be blended or reacted with linear chain homopolymers to produce composites and blends with interesting properties. A hybrid linear−dendritic diblock copolymer can be used to introduce mechanical or other desired properties of the second block, while taking advantage of molecular self-assembly to produce a nanoscale domain structure induced by the microphase separation of the two blocks. There are several published reports on the synthesis and solution behavior of linear−dendritic diblocks,[8−16] but at this time there is still much to explore regarding the solid state or thin film properties of these materials.[17] We have designed and synthesized a series of block copolymers consisting of polyamidoamine (PAMAM) dendrons attached to poly(ethylene oxide) linear chains (PEO) as described in a previous publication.[16] These materials were designed to undergo self-assembly in the bulk state, in solution, and at the air−water interface. These block copolymers can be made amphiphilic via end-group functionalization; the resulting macroamphiphiles form stable monolayers at the air−water interface of a Langmuir trough, and their LB behavior has been reported recently.[18] The monolayers undergo phase transitions when compressed and can be transferred onto hydrophobically functionalized surfaces to create relatively uniform hole-free films. Z-type multilayer films can be formed on addition of a polyelectrolyte to the subphase.[19] The behavior of dendritic macromolecules has been an area of current interest due to the high functionality of the dendrimer surface groups. Alkyl end-functionalized spherical dendrimer homopolymers have also been examined at the air−water interface by Meijer et al.,[20] and the interfacial stability and molecular conformation of benzyl ether monodendrons have also been explored by Frank and co-workers.[21,22]

The formation of multilayer films requires uniform ordering of diblocks at the air−water interface. The behavior of diblocks at the interface depends in part on the relative sizes of the linear and dendrimer blocks. Reflectivity measurements on linear diblock monolayers can provide information on the mechanism of ordering and film formation as a function of generation. Here we report the results of neutron scattering experiments conducted on monolayers of linear−dendritic diblocks. These experiments provide insight into the orientation of the diblocks at the air−water interface and the structure of the resulting monolayer. The effects of compression and dendrimer generation number will be discussed.

2. Experimental Section

2.1. Materials. Synthesis and characterization of PEO−PAMAM linear−dendritic diblock copolymers is described elsewhere.[16] Starting material is 2000 molecular weight monodisperse PEO−NH_2 (PDI = 1.04) purchased from Shearwater Polymers. The PAMAM dendrimer block was synthesized by repeated Michael addition of methyl acrylate and amidation

10.1021/ma010361e CCC: $22.00
Published on Web 12/04/2001

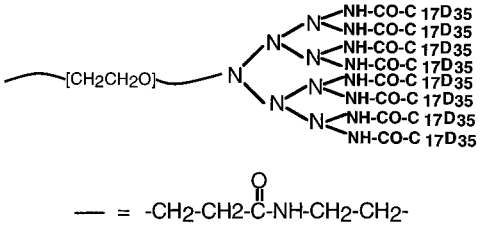

Figure 1. Schematic showing the chemical structure of PEO-(2000)−PAMAM generation 3.0-S D_{35} diblock copolymer.

with ethylenediamine in methanol. ^{1}H NMR spectra were recorded for all intermediates using a Bruker 400 instrument. FTIR spectra were also recorded using a Nicolet Magna-IR 550 spectrometer. Methyl acrylate was purchased from Aldrich and washed twice with equal amounts of 5% NaOH solution followed by two washings with Milli-Q (18.2 mΩ/ cm) water. Ethylenediamine was purchased from Aldrich and distilled before use. MALDI-TOFS data confirmed a very low polydispersity (1.01) for the PEO−PAMAM diblock copolymers synthesized using this approach. Stearate functionalization of dendrimer end groups is also described elsewhere.[18] Stearic acid is converted to its anhydride form using dicyclohexylcarbodiimide (DCC) and reacted with PAMAM in chloroform. NMR results indicate 80% of dendrimer end groups were functionalized.[18] More extensive characterization of the bulk properties of these materials will be reported in a separate paper.[23] Deuterated stearic acid was chosen to provide contrast for neutron scattering experiments. The deuterated acid was purchased from Aldrich and used without further purification.

2.2. Neutron Reflection Apparatus. Neutron reflectivity measurements were conducted at the National Institute of Science and Technology (NIST) research reactor in Gaithersburg, MD. The wavelength of the neutrons was 4.76 Å. Experiments were conducted at room temperature. The Langmuir trough was 26 by 11.4 cm and lined with poly(tetrafluoroethylene) (PTFE). It had a moveable PTFE barrier and was enclosed to prevent contamination. The trough was cleaned prior to use with ethanol and then with Milli-Q (18.2 mΩ·cm) water and dried. Milli-Q water was also used as the subphase for monolayers. The neutron beam entered and exited the trough enclosure through aluminum foil windows on opposite walls of the enclosure. A detector measured the number of neutrons exiting the trough enclosure. The entire trough enclosure could be raised and lowered to change the angle of the neutron beam path and hence the incidence angle relative to the trough surface.

2.3. Experimental Procedure. Monolayers were prepared by dissolving a known quantity of PEO−PAMAM diblock material in chloroform. The concentration of diblock was typically between 1.5 and 2.5 mg/mL. Next, a small quantity of chloroform solution, typically 20−50 μL, was deposited dropwise on the water surface using a microliter syringe. The chloroform was allowed to evaporate for 60 min prior to compression. The barrier was then moved to compress the monolayer to a surface concentration of 640 Å^2/molecule. The monolayer was given 45 min to relax after compression and then exposed to the neutron beam. Reflection data were collected for 1−2 h before closing the neutron shutter and further compressing the monolayer. This procedure was used to collect reflectivity data at surface concentrations of 640, 216, 150, and 110 Å^2/molecule for each monolayer. These surface concentrations encompassed the gas, liquid, and solid regions of the pressure−area (π−a) isotherm for the monolayer.

3. Results and Discussion

The chemical structure of a deuterated stearate-functionalized third generation linear−dendritic diblock, PEO(2K)-3.0-D, is shown in Figure 1. The water-soluble linear block was monodisperse poly(ethylene oxide) (PEO) with a molecular weight of 2000, and the dendron block was polyamidoamine (PAMAM). The amino end

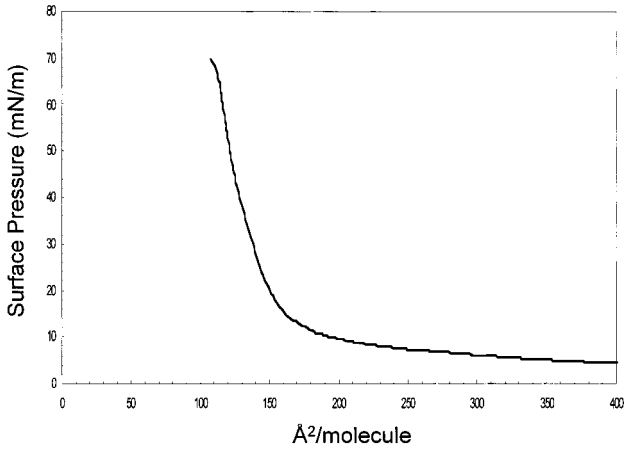

Figure 2. Pressure−area isotherm measured at 20 °C for deuterated stearate-functionalized PEO(2000) third generation PAMAM diblock monolayer on H_2O subphase.

Table 1. Area per Molecule for PEO(2000)−PAMAM Diblock Copolymers

dendrimer generation	no. of stearate groups	theor area (Å^2)	exptl area (Å^2)
0	1	20	25
2	4	80	155
3	8	160	185
4	16	320	195

groups of the PEO(2K)−PAMAM were functionalized with deuterated stearic acid to make the dendritic block surface hydrophobic; the resulting block copolymers are amphiphilic, with deuterium-labeled hydrophobic end groups (D).

In previous work, we have found that stearate-functionalized PEO−PAMAM diblock copolymers exhibit surface activity and form stable monolayers at the air−water interface,[18] which can be transferred to form thin films. A representative pressure−area isotherm for deuterated stearate-functionalized PEO(2K)-3.0-D is shown in Figure 2; the profile is very similar to that observed in the nondeuterated samples examined in previous work. The isotherm reaches a high surface pressure before collapse of the monolayer, indicating the formation of a condensed phase at the air−water interface. The observed areas per molecule are consistent with the arrangements of the macroamphiphiles perpendicular to the interface and do not indicate the formation of surface aggregates or micelles. Previous work on these systems has also indicated that surface micelle formation does not occur for generations 2.0 and higher.[19] Evidence of the presence of surface micelles was only observed for the functionalized generation 1.0 PEO−PAMAM diblock copolymer, as reported earlier. In general, other studies of monodendrons, spherical dendrimers, and dendritic diblocks have also shown no indications of aggregation of the dendrons during compression.[20,22,24] Extrapolation of the slope of the isotherm prior to the collapse point yields the area per molecule for the macroamphiphile when packed in the dense solid phase. The surface area per molecule can be estimated on the basis of the area taken up by each stearate end group for the dendritic block. The areas calculated on the basis of the area of the stearate end groups are compared with the actual experimental values in Table 1. For stearate terminated PEO(2K)-G2.0-S, the area per molecule exceeded the net molecular cross-sectional area of the attached stearate groups, assuming that the

stearate groups are fully extended and oriented perpendicular to the water subphase, as is observed with stearic acid. This phenomenon was attributed to the presence of the PEO block at the air−water interface even at very high pressures and low areas. It was proposed that the PEO tail, which is also slightly surface active, finds its way around the relatively small dendron block and is expressed at the surface; thus, the lower generation systems may exist as monolayers with a moderate concentration of PEO segments present in the layer. The intercolation of PEO at the surface prevents close packing of the dendritic block when compressed at the air−water interface.

On the other hand, the area per molecule observed for the third generation dendrimer much more closely approximated that expected for eight stearic acid groups at the air−water interface. At the third generation, the estimated radius of gyration of the PEO block in water is about the size of the dendron block; therefore, fewer PEO segments extend beyond the dendron to access the air−water interface in this case. The stearate groups are presumed to occupy the top portion of the monolayer, existing as an ordered alkyl array. Finally, the area per molecule of functionalized fourth generation PEO(2K)−PAMAM was actually less than the expected area of the attached stearate groups, despite NMR evidence in previous work that the end groups on this block are almost completely functionalized. In this case, the shape of the fourth generation dendrimer is believed to prevent complete organization of the stearate groups normal to the air−water interface. The surface formed by the branch ends of fourth generation PAMAM may be sufficiently curved that the attached stearate groups disorder or intermix when compressed at the air−water interface. The lack of ordered stearate groups may allow further compression of the underlying dendron block, ultimately leading to buckling at the interface to yield an area per molecule which is less than that required if all the stearate groups were uniformly oriented at the air−water interface. There is evidence that dendrimers are highly compressible and will deform at high pressures at the air−water interface.[20,24] It was thus proposed that compression of third generation dendritic diblocks yields highly ordered stearate groups at the air−water interface, whereas compression of fourth generation diblocks results in a disordered layer with intermixed stearate groups and dendritic blocks in a buckled arrangement at the surface. The less ordered stearate system exhibits a higher degree of compressibility and probable large deformation of the dendron block.[18,19]

To further understand ordering at the air−water interface, neutron reflectivity experiments have been conducted on monolayers of deuterated amphiphilic linear dendritic diblock copolymers to determine how the monolayer structure varies with surface area per molecule and the generation of the dendrimer. The deuterated stearate block copolymers were spread on a Langmuir trough configured to allow the collection of neutrons reflected from the air−water interface at various points along the pressure−area isotherm. The angle was varied by lowering the trough table stepwise during data collection. Neutron reflectivity is described in detail by Lekner[25] and Born and Wolf.[26] Reflectivity applications for polymers are described by Russell[27] and Thomas.[28] The specular neutron reflection experiments described here were modeled using the optical matrix method and the Spreadsheet Environment Reflectivity Fitting (SERF) software developed by Welp, Co., and Wool at the University of Delaware.[29] In this approach the monolayer is described as layers of PEO, PAMAM, and stearate groups. Modeling was accomplished by changing the thickness and composition of the layers to match experimental data. Specular reflectivity was calculated using the software and the thickness and composition of the individual layers of the model. Data were collected on both D_2O and H_2O subphases for generations 3 and 4 in this study.

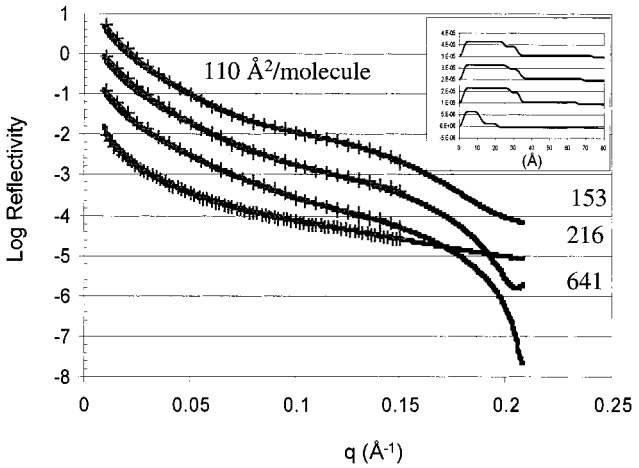

Figure 3. Experimental reflectivity profiles and model results for deuterated stearate-functionalized PEO(2000) third generation PAMAM diblock monolayer on H_2O subphase. Surface concentration ranges from 641 to 110 Å²/molecule. Curves are shifted vertically to prevent overlap. The inset shows the corresponding scattering length density profiles with the horizontal axis representing the direction normal to the monolayer surface. Scattering length density profiles are also shifted vertically to prevent overlap.

Reflectivity on an H_2O Subphase. The data for PEO(2K)-3.0-D on an H_2O subphase were collected at four different points of compression, with each corresponding to different surface areas: 641, 216, 153, and 110 Å²/molecule, with increasing surface pressure. These surface areas correspond to the expanded "gas", liquidlike, transitional, and solid regions of the typical pressure area isotherm from this system. As a point of reference, the undeuterated stearate third generation diblock copolymer, which has eight end groups, exhibited a packed monolayer at 185 Å²/molecule, whereas the area taken up by eight stearic acid groups alone is 160 Å²/molecule. Figure 3 shows the experimental reflectivity profiles and model results for a monolayer composed of a diblock with 2000 molecular weight linear PEO and deuterated stearate-functionalized third generation PAMAM dendrimer. A layer model was used to fit data for each of the reflectivity profiles, with variations in the composition and thicknesses of the layers for each profile. The layered model for monolayers correlates well to the experimental data. The inset in Figure 3 shows the scattering length density profiles corresponding to the models used to calculate the reflectivity profiles for each surface compression level. It is noted that in all cases these models represent a best fit to the data using the slab model approach. The slabs comprising the model are based on our understanding of the surface pressure−area isotherms obtained from previous work. The resulting models have allowed us to make qualitative comparisons of the film

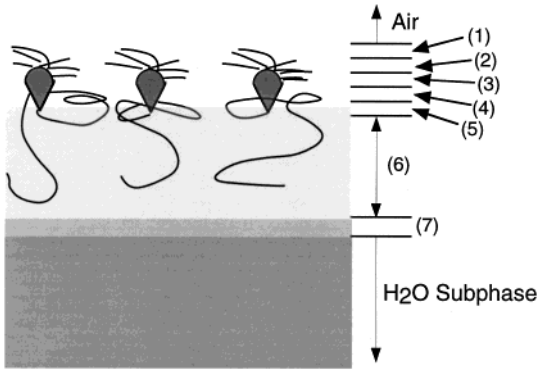

Figure 4. Schematic diagram of layered model used to calculate reflectivity for the third generation stearate-functionalized linear−dendritic diblock copolymer monolayer corresponding to a surface concentration of 640 Å^2/molecule. Model corresponds to experimental results for tests lasting 8 h. The various layers of the model are as follows: (1) 4 Å interfacial gradient between air and stearate groups, (2) 5 Å thick layer composed entirely of stearate groups, (3) 5 Å thick interfacial gradient, (4) 5 Å thick layer composed of 20% PAMAM dendrimer and 80% PEO, (5) 4 Å thick interfacial gradient, (6) 42 Å thick layer composed of 10% PEO and 90% H_2O, and (7) 6 Å thick interfacial gradient.

order and composition observed in each of the systems examined.

The model chosen to fit the data for a molecular surface area of 640 Å^2/molecule is shown in Figure 4. The surface pressure is independent of surface concentration, and the monolayer is approaching the gaseous region of the $\pi-a$ isotherm. The top of the model monolayer is a 4 Å error function composition gradient representing roughness in the monolayer surface. Beneath this gradient is a 5 Å thick region composed entirely of hydrophobic stearate groups. Next there is a 5 Å composition gradient separating the stearate layer from a 5 Å thick layer composed of 20% PAMAM dendrimer and 80% PEO. Below the dendrimer-containing layer is a 4 Å composition gradient which rests above a 42 Å thick layer containing 10% PEO and 90% H_2O. The bottom portion of the model monolayer is a 6 Å error function gradient between the 10% PEO layer and the H_2O subphase. From the model shown in Figure 4, there is evidence that the stearate groups exist primarily at the top of the monolayer, where they would best minimize interfacial free energy at the air interface. The extended chain length of a stearate group is much greater than the 5−9 Å thickness of the stearate layer in the model, indicating that the stearate groups probably lie along the surface of the monolayer at this surface concentration. It is expected that the monolayer would be relatively thin, as the stearate groups spread as much as possible across the water phase to lower interfacial tension, which is often observed with fatty acids at low pressures. Because PEO is slightly surface active, it is suggested that the number of PEO segments present at the interface between the stearate groups and water is relatively large, as illustrated by the PEO/PAMAM ratio in the second layer. The PEO can act to lower the interfacial free energy between the hydrophobic alkyl groups and water. The low amount of PEO in the water phase of this model implies that the PEO is concentrated at the interface at low surface pressures, consistent with commonly observed experimental studies of PEO homopolymers. The PAMAM dendrimer groups are modeled as a separate layer from the stearate groups, suggesting that the PAMAM is fairly well excluded from the hydrophobic alkyl tails; on the other hand, the dendron does appear to mix to some extent with the PEO block.

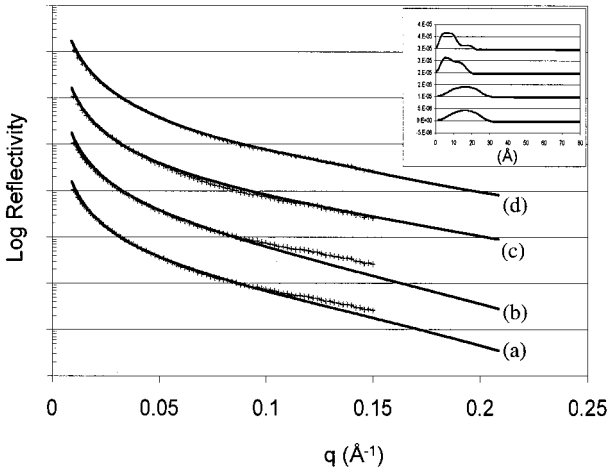

Figure 5. Experimental reflectivity profiles and model results for deuterated stearate-functionalized PEO(2000) third generation PAMAM diblock monolayer on H_2O subphase at 641 Å^2/molecule. Models represent various degrees of intermixing of polymer blocks: (a) fully intermixed monolayer lacking any internal structure; (b) monolayer with an upper internal layer which is fully intermixed and lower internal layer consisting of 40% PEO and 60% H_2O; (c) monolayer in which stearate groups form a distinct layer above an intermixed layer; (d) monolayer with three distinct layers, same as 641 Å^2/molecule curve in Figure 3. Inset shows corresponding scattering length density profiles for the model monolayers shifted vertically to prevent overlap.

It is somewhat surprising that the PEO, PAMAM, and stearate groups comprising the monolayer model described above would be segregated into distinct layers at a surface concentration of 640 Å^2/molecule. One might expect, for example, that the linear polymer would penetrate the voids of the dendritic block. However, the segregated monolayer structure suggests that microphase segregation is occurring at the interface, much as it is observed in the bulk state lamellar morphologies of this polymer.[23] Several models that involve the intermixing of polymer blocks were investigated in this work. Figure 5 shows several examples of model reflectivity profiles for the 640 Å^2/molecule case with varying degrees of intermixing. It is evident that the reflectivity model for a fully intermixed monolayer lacking any layered internal structure (Figure 5, curve a) does not match the experimental data at 640 Å^2/molecule. Also shown is a model reflectivity profile for a monolayer with two internal layers consisting of a top layer which is a mixture of 40% stearate, 30% PAMAM, and 30% PEO and a lower layer mixture of 40% PEO and 60% H_2O (Figure 5, curve b). This profile corresponding to a hydrogenated PEO layer beneath an intermixed layer fails to match experimental data for $q > 0.1$ nm^{-1}. The reflectivity profile corresponding to monolayer structure with a stearate layer above the intermixed layer (Figure 5, curve c) fits experimental data better than either the intermixed monolayer or the one with a PEO layer beneath the intermixed layer; however, it deviates from the experimental data in the range $0.05 < q < 0.1$ nm^{-1}. The best fit to experimental data for the 640 Å^2/molecule case is the one in which the stearate, PAMAM, and PEO blocks each form distinct layers (Figure 5, curve d), which was presented in the previous figures.

Effect of Compression. The density profiles in Figure 3 illustrate the gradual change in ordering of

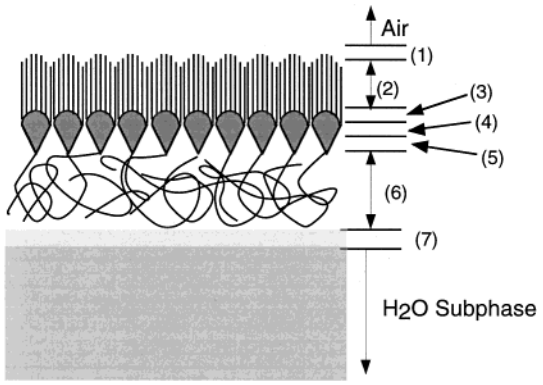

Figure 6. Schematic diagram of layered model used to calculate reflectivity for the third generation stearate-functionalized linear−dendritic diblock copolymer monolayer corresponding to a surface concentration of 110 Å^2/molecule. The various layers of the model are as follows: (1) 4 Å interfacial gradient between air and stearate groups, (2) 19 Å thick layer composed entirely of stearate groups, (3) 3 Å thick interfacial gradient between stearate and PAMAM, (4) 4 Å thick layer composed entirely of PAMAM, (5) 4 Å thick interfacial gradient between PAMAM and PEO, (6) 37 Å thick layer composed entirely of PEO, and (7) 5 Å thick interfacial gradient between PEO and subphase.

the dendritic macroamphiphiles upon compression of the Langmuir monolayer. As the surface pressure is increased, the various layers in the model corresponding to the stearate, PAMAM, and PEO portions of the monolayer become thicker and more distinct. As the surface area per molecule decreases from 641 to 216 Å^2/molecule, the thickness of the stearate layer increases from 5 to 19 Å, which corresponds well to the extended length of the stearate groups. The thickness of the PEO layer also increases, undergoing significant change from 28 to 37 Å, when the surface area is decreased from 216 to 110 Å^2/molecule. The PAMAM layer undergoes a more subtle increase in thickness with surface concentration, presumably as it is excluded from mixing with the PEO phase at high surface concentrations. Modeling indicates that the composition gradients corresponding to interfacial regions and surface roughness do not change significantly during compression. In all cases the monolayers were given 45 min to relax at constant surface pressure prior to collecting reflectivity data. Changes in the interfacial roughnesses are not very marked following this relaxation period. This phenomenon may be an indication that the monolayer has reached a psuedostable state at each surface pressure prior to collection of reflectivity data. It is also worth noting that in the bulk state PEO−PAMAM dendritic diblocks exhibit phase segregation; it is probable that similar segregation occurs on the surface at high pressures, as the macromolecules become more compressed and ordered.

Figure 6 shows the layer model used to calculate the reflectivity profile shown in Figure 3 for a surface concentration of 110 Å^2/molecule. In this case the monolayer is at its most compressed state corresponding to the solid region of the $\pi-a$ isotherm. The top of this monolayer is a 4 Å thick layer in which the material composition varies from that of air to stearate groups. This layer represents the surface roughness of the monolayer. The next layer is 19 Å thick and composed entirely of stearate groups. This model suggests a transition from planar arrangements to the perpendicular packing of ordered arrays of stearate groups on the monolayer surface at high surface pressure. The composition of this layer does not vary spatially. Below the stearate layer is a 3 Å thick error function composition gradient followed by a 4 Å thick layer composed entirely of PAMAM dendrimer. A 4 Å thick error function composition gradient separates the PAMAM layer from the PEO layer. The PEO layer is 37 Å thick and composed entirely of PEO. Beneath the PEO layer is a 5 Å thick composition gradient of PEO and water and finally the H_2O subphase.

As noted above, the thickness of the stearate layer indicates that these groups extend vertically from the monolayer surface. The thickness of the PAMAM layer plus the adjacent two composition gradients is close to the hydrodynamic radius of spherical PAMAM dendrimers obtained from viscosity measurements[30] in water (R_h = 14.6 Å) and methanol (R_h = 15.3 Å) and neutron scattering measurements[31] in methanol of second generation PAMAM homopolymers. Second generation PAMAM homopolymers contain dendrons with the same number of repeat units and end groups (eight) as the dendrons in the third generation PEO−PAMAM diblocks studied here; thus, the length scale of the PAMAM layer is consistent with that of a similarly branched dendritic structure. Although the model suggests a pure PAMAM layer, it is expected that the dendron would be somewhat hydrated near the air−water interface due to its hydrophilic nature; however, it should be noted that the stearic acid groups are very hydrophobic and may shield the dendron from water adsorption, particularly at high pressures. Reflectivity data were taken from two successive 1 h tests at 110 Å^2/molecule; the reflectivity profiles of each data set overlap, indicating that no observable change occurred in the monolayer during testing.

The thickness of the PEO layer in Figure 6, 37 Å, is close to the calculated radius of gyration for 2000 molecular weight PEO in water. Surprisingly, the best fit to the layer model suggests that the composition of the PEO layer does not vary spatially and consists entirely of PEO. Given the water-soluble nature of PEO, this result was not initially expected. However, there are several published reports describing both diblock copolymers and homopolymers in which PEO chains form films resting on a water surface.[32−36] The behavior of PEO differs from other hydrophilic polymers because the ethylene glycol monomer repeat is itself amphiphilic and is attracted to hydrophobic surfaces when dissolved in water. This attraction brings the PEO to the air−water interface. Faure et al. studied $\pi-a$ isotherms of PEO−PS diblocks and found that the PEO block initially forms a quasi-two-dimensional layer. Upon compression, the PEO begins to desorb from the interface and form short brushes in the subphase. The onset of brush formation corresponded to the appearance of a plateau in the $\pi-a$ isotherm and was associated with competition between the water solubility of the EO monomer units and their attraction to the surface. Isotherms of PEO−PAMAM linear−dendritic block copolymers do not exhibit the plateau associated with brush formation over the compression range studied here. The absence of a plateau may be due to the relatively low molecular weight of the PEO chains used here. Shuler and Zisman[35] examined the behavior of PEO homopolymers at the air−water interface and concluded that water molecules bound to the polymer chain would cause the PEO to adopt a more expanded conformation and increase its limiting area per mol-

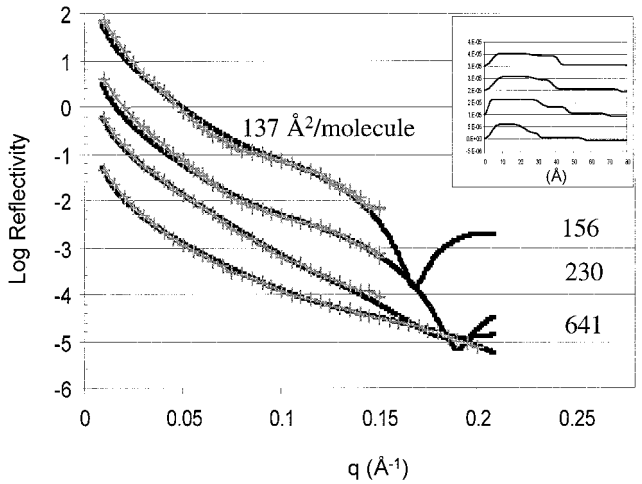

Figure 7. Reflectivity profile and model results for deuterated stearate-functionalized PEO(2000) fourth generation PAMAM diblock monolayer on H_2O subphase. Surface concentration ranges from 641 to 137 Å^2/molecule. Curves are shifted vertically to prevent overlap. Inset shows corresponding scattering length density profiles for model monolayers shifted vertically to prevent overlap.

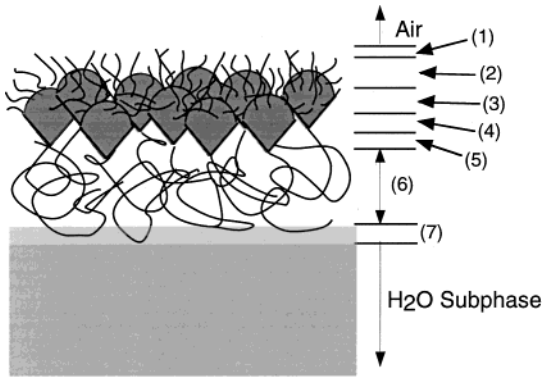

Figure 8. Schematic diagram of layered model used to calculate reflectivity for the fourth generation stearate-functionalized linear−dendritic diblock copolymer monolayer corresponding to a surface concentration of 137 Å^2/molecule. The various layers of the model are as follows: (1) 8 Å interfacial gradient between air and stearate groups, (2) 12 Å thick layer composed of 50% stearate groups and 50% PAMAM, (3) 12 Å thick interfacial gradient between stearate and PAMAM, (4) 7 Å thick layer composed entirely of PAMAM, (5) 4 Å thick interfacial gradient between PAMAM and PEO, (6) 35 Å thick layer composed entirely of PEO, and (7) 4 Å thick interfacial gradient between PEO and subphase.

ecule. They claimed that by excluding water the PEO chain could adopt a more compact conformation to help it remain at the air−water interface through the liquid and solid regions of the $\pi-a$ isotherm. The reduction in surface tension when PEO formed a monolayer at the air−water interface was sufficient to overcome the hydrophilic interactions of the EO repeat units as the monolayer was compressed. For the PEO−PAMAM diblocks discussed here, it is possible that the PEO block can best accommodate the monolayer structure of ordered stearate groups by adopting a more compact conformation, thus excluding water. Modeling results for the reflectivity profiles shown in Figure 3 for surface concentrations of 216 and 153 Å^2/molecule also indicate that the PEO forms a distinct layer on top of the H_2O subphase. However, the reflectivity model for the PEO layer shown in Figure 4 consists of 90% H_2O, at a surface concentration of 640 Å^2/molecule. In this case the data collection lasted approximately 10 h, while all the other tests in which the PEO was found to be on top of the H_2O subphase lasted 2−3 h. For this reason, we cannot rule out the possibility that the PEO chains become solvated in the subphase if given sufficient time.

Effect of Dendrimer Generation. Figure 7 shows experimental and model reflectivity profiles for a monolayer of deuterated stearate-functionalized fourth generation PEO−PAMAM. The surface concentration for this monolayer varies from 641 to 137 Å^2/molecule. The inset of Figure 7 shows the scattering length density profiles corresponding to the calculated reflectivity profiles. The scattering length density profiles in Figure 7 for the fourth generation monolayer share several characteristics with the profiles for the third generation shown in Figure 3. In both cases, the model used proposes that the stearate groups lie flat on the monolayer surface at 640 Å^2/molecule and extend upon further compression. In addition, the PEO layer becomes thicker and no longer intermixes with PAMAM upon compression for both the third and fourth generation.

Figure 8 shows the model monolayer used to the calculate the reflectivity and density profiles in Figure 7 at high surface pressure at a surface concentration of 137 Å^2/molecule. The top layer of this model is an 8 Å thick composition gradient representative of surface roughtness. Below this is a 12 Å thick mixed layer composed of 50% stearate groups and 50% PAMAM. Next is a 12 Å thick composition gradient atop a 7 Å thick layer of 100% PAMAM. Below the PAMAM is a 5 Å thick composition gradient. Next is the PEO layer, which is 35 Å thick and composed of 100% PEO, as was observed for the third generation diblock as well. Finally, there is a 4 Å composition gradient and the H_2O subphase.

The major difference between the third and fourth generation is that the density profiles suggest that the stearate and dendrimer layers are intermixed, as described by the model. In models for the third generation monolayer the stearate layer is composed entirely of stearate groups and sits above the PAMAM layer. In models for the fourth generation the stearate layer is a mixture of stearate and PAMAM whose composition varies with surface concentration. In addition, the interfacial region between the stearate and fourth generation PAMAM layers is 2−3 times thicker than third generation at all surface concentrations. This intermixing of stearate groups and PAMAM is believed to occur because the outer edge of the fourth generation dendrimer has significant curvature. In this case the tendency for the stearate groups to form a uniform layer of extended chains is countered by their attachment to the nonplanar dendron surface. In the absence of a well-oriented alkyl monolayer at the surface, it appears that compression of the dendron is facilitated at higher surface pressures. On the basis of these observations, compression appears to cause the dendron monolayer to buckle or distort to accommodate the disordered stearate groups, creating what appears to be intermixing of PAMAM and stearate groups. This is consistent with LB isotherm measurements of the area per molecule of PEO−PAMAM G4.0-S monolayers. LB measurements showed that the area per diblock molecule was less than the combined cross-sectional area of the stearate groups attached to the dendrimer. The cross-section area of stearate groups was assumed to be the

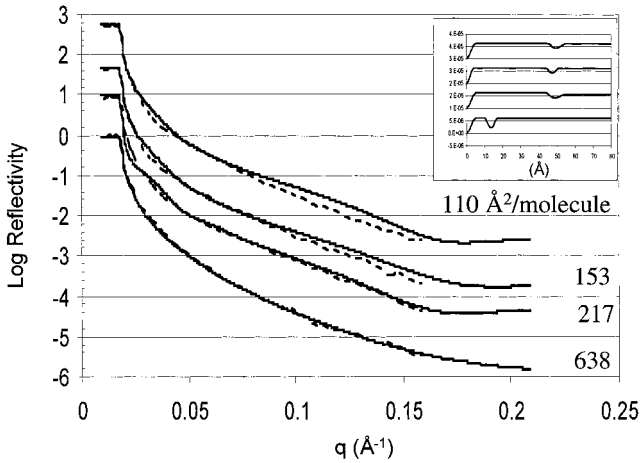

Figure 9. Experimental reflectivity profiles and model results for deuterated stearate-functionalized PEO(2000) third generation PAMAM diblock monolayer on D_2O subphase. Surface concentration ranges from 638 to 110 Å^2/molecule. Curves are shifted vertically to prevent overlap. Inset shows the corresponding scattering length density profiles for the model monolayers shifted vertically to prevent overlap.

area per molecule of stearic acid monolayers measured on an LB trough.

The dendrimer layer is thicker for the fourth generation than for the third. The combined thickness of the fourth generation dendrimer layer plus the two composition gradients which separate it from the stearate and PEO layers is about 20 Å at all surface concentrations. This value is close to the hydrodynamic radius measured in H_2O and the radius of gyration determined from neutron scattering experiments in H_2O and CH_3OH on PAMAM homopolymers with the same size dendron groups. Increasing the dendrimer generation from 3.0 to 4.0 increases the thickness of the PAMAM layer by an amount that is consistent with the published hydrodynamic radius for PAMAM homopolymers.

Effect of Deuterated Subphase. Reflectivity experiments were conducted using deuterium oxide, D_2O, as the subphase for diblock monolayers of deuterated stearate-functionalized third generation PAMAM−PEO diblocks. Figure 9 shows the reflectivity profiles and model results for deuterated stearate-functionalized third generation PAMAM−PEO diblock monolayers on D_2O at surface pressures ranging from 638 to 110 Å^2/molecule. The inset of Figure 9 shows the corresponding scattering length density profiles. Unlike the experiments done with an H_2O subphase, the model did not fit the experimental data as well at higher pressures. The corresponding scattering length density profiles based on these models do not correlate as well to the expected molecular dimensions of the monolayer; in general, discrepancies between the calculated model layer and the predicted molecular scale thicknesses of up to 50−100% were observed, making these results less realistic with respect to the actual chain lengths.

We believe that the dominance of the reflection by the D_2O subphase is the cause of these anomalies; unfortunately, for this reason the results from the deuterated subphase are not representative of a realistic model. Richards, Rochford, and Webster[33] also used neutron reflectivity to examine PEO−PMMA diblocks spread as monolayers on D_2O and found that the strong reflection from D_2O obscures the monolayer. This research group indicated that these reflections prevented a reasonable analysis of the data. Results from the D_2O subphase show that in the best-fit models the stearate groups lie parallel to the monolayer surface when the surface concentration is 638 Å^2/molecule, and stearate orientation is perpendicular to the surface upon further compression, as was observed for third and fourth generation monolayers on the H_2O subphase. Overall, the data set from the deuterated subphase is qualitatively consistent with our results on the PAMAM and stearate organization obtained from the H_2O subphase.

4. Summary and Conclusions

Specular reflection of neutrons has been used to investigate the structure of monolayers composed of alkyl-terminated linear−dendritic diblock copolymers in an LB trough. The linear block consisted of 2000 molecular weight PEO, and the dendrimer block consisted of PAMAM generation 3.0 and 4.0 functionalized with deuterated stearate groups. Results based on a slab model of the alkyl functional PAMAM−PEO diblock copolymers indicate that the stearate groups segregate to the top surface of the monolayer at low and high surface pressures. The model neutron reflectivity density profiles suggest that the PEO segments rest on top of the H_2O surface as a separate layer, particularly at very high surface pressures. As the monolayer is compressed and the diblocks become more crowded on the surface, the stearate groups rearrange from a flat planar conformation to a lateral fully extended one, thus minimizing interfacial free energy with the air interface. The PEO excludes the PAMAM groups as surface concentration increases, eventually forming distinct PEO and PAMAM layers. It is proposed that generation 4.0 PAMAM exhibits surface curvature. As a result, the stearate groups cannot form a well-ordered phase oriented perpendicular to the interface, resulting in a disordered and partially mixed stearate layer and lower than expected area per molecule based on the number of branches on the dendron. These data confirm earlier reported data on the Langmuir−Blodgett behavior of these systems.[18]

Acknowledgment. Financial support for this work came from the Environmental Protection Agency (Grant R825224-01-1). The authors thank Kaler for use of the SERF software.

References and Notes

(1) Matthews, O. A.; Shipway, A. N.; Stoddart, J. F. *Prog. Polym. Sci.* **1998**, 1−56.
(2) Jansen, J. F. G. A.; de Brabaamder-van den Berg, E. M. M.; Meijer, E. W. *Science* **1994**, *266*, 1226−1229.
(3) Zhao, M.; Sun, L.; Crooks, R. M. *J. Am. Chem. Soc.* **1998**, *120*, 4877−4878.
(4) Balogh, L.; Tomalia, D. A. *J. Am. Chem. Soc.* **1998**, *120*, 7355−7356.
(5) Tokuhisa, H.; Crooks, R. M. *Langmuir* **1997**, *13*, 5608−5612.
(6) Bardaji, M.; Kustos, M.; Caminade, A.-M.; Majoral, J.-P.; Chaudret, B. *Organometallics* **1997**, *16*, 403−410.
(7) Alonso, E.; Valerio, C.; Ruiz, J.; Astruc, D. *New J. Chem.* **1997**, *21*, 1139−1141.
(8) Fréchet, J. M. J.; Hawker, C. J.; Wooley, K. L. *Pure Appl. Chem.* **1994**, *A31*, 1627−1645.
(9) Gitsov, I.; Fréchet, J. M. J. *Macromolecules* **1993**, *26*, 6536−6546.
(10) Gitsov, I.; Wooley, K. L.; Hawker, C. J.; Ivanova, P. T.; Fréchet, J. M. J. *Macromolecules* **1993**, *26*, 5621−5627.
(11) Hawker, C. J.; Wooley, K. L.; Fréchet, J. M. J. *J. Chem. Soc., Perkin Trans. 1* **1993**, 1287.
(12) van Hest, J. C. M.; Baars, M. W. P. L.; Elissen-Roman, C.; van Genderen, M. H. P.; Meijer, E. W. *Macromolecules* **1995**, *28*, 6689−6691.

(13) Chapman, T. M.; Hillyer, G. L.; Mahan, E. J.; Shaffer, K. A. *J. Am. Chem. Soc.* **1994**, *116*, 11195.
(14) de Brabander-van den Berg, E. M.; Meijer, E. W. *Angew. Chem., Int. Ed. Engl.* **1993**, *32*, 1308−1311.
(15) Aoi, K.; Motoda, A.; Okada, M. *Macromol. Rapid Commun.* **1997**, *18*, 945−952.
(16) Iyer, J.; Hammond, P. T. *Macromolecules* **1998**, *31*, 8757−8765.
(17) Roman, C.; Fischer, H. R.; Meijer, E. W. *Macromolecules* **1999**, *32*, 5525−5531.
(18) Iyer, J.; Hammond, P. T. *Langmuir* **1999**, *15*, 1299−1306.
(19) Iyer, J. Doctoral Dissertation, Chemical Engineering Department, Massachusetts Institute of Technology, Cambridge, MA, 1999.
(20) Schenning, A.; Elissen-Roman, C.; Weener, J. W.; Baars, M.; van der Gaast, S. J.; Meijer, E. W. *J. Am. Chem. Soc.* **1998**, *120*, 8199−8208.
(21) Frank, C. W.; Kampf, J. P.; Malmström, E. E.; Hawker, C. J. *Abstr. Pap. Am. Chem. Soc.* **1999**, *217*, 101-PMSE.
(22) Kampf, J. P.; Frank, C. W.; Malmström, E. E.; Hawker, C. J. *Langmuir* **1999**, *15*, 227−233.
(23) Johnson, M. A.; Hammond, P. T., manuscript in preparation.
(24) Saville, P. M.; Reynolds, P. A.; White, J. W.; Hawker, C. J.; Fréchet, J. M. J.; Wooley, K. L.; Penfold, J.; Webster, J. R. P. *J. Phys. Chem.* **1995**, *99*, 8283−8289.
(25) Lekner, J. L. *Theory of Reflection*; Martinus Nijhoff Publishers: Dodrecht, 1987.
(26) Born, M.; Wolf, E. *Principles of Optics*; Pergamon: Oxford, U.K., 1980.
(27) Russell, T. P. *Mater. Sci. Rep.* **1990**, *5*, 171−271.
(28) Thomas, R. K. *Scattering Methods in Polymer Science*; Ellis Horwood Publishers: New York, 1995.
(29) Welp, K. A.; Co, C. C.; Wool, R. P. *J. Neutron Res.*, in press.
(30) Stechemesser, S.; Eimer, W. *Macromolecules* **1997**, *30*, 2204−2206.
(31) Bauer, B. J.; Topp, A.; Prosa, T. J.; Amis, E. J.; Yin, R.; Qin, D.; Tomalia, D. A. *Abstr. Pap. Am. Chem. Soc.* **1997**, *214*.
(32) Li, Z.; Zhao, W.; Quinn, J.; Rafailovich, M. H.; Sokolov, J.; Lennox, R. B.; Eisenberg, A.; Wu, X. Z.; Kim, M. W.; Sinha, S. K.; Tolan, M. *Langmuir* **1995**, *11*, 4785−4792.
(33) Richards, R. W.; Rochford, B. R.; Webster, J. R. P. *Polymer* **1997**, *38*, 1169−1177.
(34) Cox, J. K. Y.; K.; Eisenberg, A.; Lennox, R. B. *Phys. Chem., Chem. Phys* **1999**, *18*, 4417−4421.
(35) Shuler, R. L.; Zisman, W. A. *J. Phys. Chem.* **1970**, *74*, 1523−1534.
(36) Faure, M. C.; Bassereau, P.; Carignano, M. A.; Szleifer, I.; Gallot, Y.; Andelman, D. *Eur. Phys. J. B* **1998**, 365−375.

MA010361E